

Journal Pre-proofs

Experimental and numerical characterization of titanium-based fibre metal laminates

Nassier.A. Nassir, R.S. Birch, W.J. Cantwell, D. Rico Sierra, S.P. Edwardson, G. Dearden, Z.W. Guan

PII: S0263-8223(20)30574-2

DOI: <https://doi.org/10.1016/j.compstruct.2020.112398>

Reference: COST 112398

To appear in: *Composite Structures*

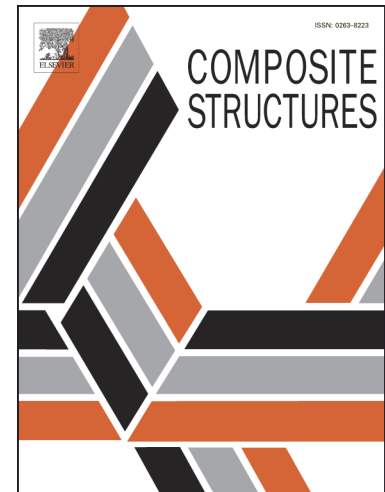
Received Date: 7 February 2020

Accepted Date: 17 April 2020

Please cite this article as: Nassir, Nassier.A., Birch, R.S., Cantwell, W.J., Rico Sierra, D., Edwardson, S.P., Dearden, G., Guan, Z.W., Experimental and numerical characterization of titanium-based fibre metal laminates, *Composite Structures* (2020), doi: <https://doi.org/10.1016/j.compstruct.2020.112398>

This is a PDF file of an article that has undergone enhancements after acceptance, such as the addition of a cover page and metadata, and formatting for readability, but it is not yet the definitive version of record. This version will undergo additional copyediting, typesetting and review before it is published in its final form, but we are providing this version to give early visibility of the article. Please note that, during the production process, errors may be discovered which could affect the content, and all legal disclaimers that apply to the journal pertain.

© 2020 Published by Elsevier Ltd.



Experimental and numerical characterization of titanium-based fibre metal laminatesNassier. A. Nassir^{a,b}, R.S. Birch^b, W. J. Cantwell^c, D. Rico Sierra^b, S. P. Edwardson^b, G. Dearden^b andZ.W. Guan^{*b,d}

a Department of Materials Engineering, University of Technology, Baghdad, Iraq

b School of Engineering, University of Liverpool, Liverpool L69 3GQ, UK

c Department of Aerospace Engineering, Khalifa University of Science and Technology (KUST), P.O. Box 127788, Abu Dhabi, United Arab Emirates.

d School of Mechanical Engineering, Chengdu University, Shiling Town, Chengdu City, Sichuan Province, P.R. China

Abstract

The effect of applying a laser surface treatment to the metal plies in a fibre metal laminate (FML) based on a titanium alloy and a fibre reinforced composite has been evaluated and the response compared to that measured on a comparable untreated laminate. It has been shown that applying a laser fluence of 4.54 J/cm² to the titanium layers in the FML results in a good bond strength between the titanium foil and the glass fibre/PEKK composite. The response of the FMLs under dynamic loading was studied and compared with that measured at quasi-static rates. It has been shown that FMLs based on a titanium alloy exhibit a rate-sensitivity, both in terms of energy absorption and the maximum impact force. An examination of cross-sections removed from samples following testing at dynamic and quasi-static loading rates indicated that the FMLs absorbed energy through plastic deformation, tearing of the metal layers, delamination and fibre fracture. Finite element models were then developed to simulate the response of the FMLs under impact loading. The simulated results were validated against the corresponding experimental data by comparing both the load-displacement traces as well as the resulting failure modes, with good agreement being observed in most cases.

Key words: Titanium alloy; Fibre metal laminates; Poly-ether-ketone-ketone (PEKK); Laser treatment; Impact; Finite element

*Corresponding author: Z.W. Guan, Email: zguan@liverpool.ac.uk

1 Introduction

Fibre metal laminates (FMLs) are hybrid materials based on combinations of a metal alloy and a fibre-reinforced composite material, which were developed at Delft University of Technology in late 1970s [1]. The particular interest in using these hybrid materials is linked to their attractive properties, such as high strength/weight ratio, cost-effectiveness, ability to tailor material properties, and good fatigue, impact and corrosion resistance. FMLs have attracted significant interest from the aerospace industry in recent years, finding extensive use in certain aircraft designs, such as the upper fuselage of the Airbus A380 aircraft [2]. Based on the nature of the polymer composite, these laminates can be defined as GLARE (glass laminate aluminium reinforced epoxy), CARALL (carbon reinforced aluminium laminate), and ARALL (Aramid reinforced aluminium laminates). A number of researchers have also shown that FMLs offer attractive properties when subjected to dynamic loading, such as that associated with localized impact loading [3-5].

Surface treatment on the aluminium alloys used in FMLs is crucial to maintain the bonding strength between the metal and fibre reinforced composite. Reyes and Cantwell [5] studied the mechanical properties of FMLs based on aluminium and a tough glass fibre reinforced polypropylene. Their results showed that by introducing a level of surface roughness on the aluminium layers and inserting a resin film at the interface between the aluminium alloy and the composite layer, the interfacial fracture energy of these laminates could be significantly increased. Zhou [6] applied a chemical etching technique to treat the surface of aluminium alloys (6061-O, 6065-T6) in order to enhance their bonding characteristics before they were used to manufacture FMLs. Gonzalez-Ganche et al. [7] used three surface treatments to improve the bonding behaviour between 5052-H32 aluminium alloy and polypropylene (PP), which included a degreasing procedure, sanding treatment and a chemical bath. The results showed that the treatment of the metal layers by a sodium hydroxide and nitric acid pickling process enhanced the degree of adhesion.

However, the maximum service temperature of PP-based FMLs is a little over 80 °C. Also, there are concerns concerning the use of epoxy-based composites in the manufacture of FMLs, i.e. their resistance to fire, where the generation of smoke and toxic fumes can pose a serious health hazard [8-11]. In this regard, there is potential for using thermoplastic composites with a high operational temperature in aerospace applications, such as in the design of supersonic aircraft, where the structure may be subjected to relatively high temperatures for a long period of time. FMLs based on either poly-ether- ether -ketone (PEEK) or poly-ether ketone-ketone (PEKK) and

titanium have been considered as suitable candidates for use in such high-temperature environments [12–14]. PEKK is a tough thermoplastic that offers the advantage that its processing temperature is lower than PEEK whereas its glass transition temperature (T_g) is higher [15].

Titanium alloys offer attractive properties, such as an excellent resistance to corrosion and a good strength to weight ratio. If they are to be used in FMLs, issues relating to the ability to bond polymers to them still need to be resolved. The nature of the surface treatment applied to the metal surface has been shown to have a great effect on controlling the bonding behaviour [16]. Recently, a variety of surface treatments have been used with different degrees of success to enhance the surface texture of titanium alloys prior to bonding, these being mechanical [12, 17, 18], chemical [19], electrochemical [20], plasma surface treatments [21]. Although, investigations of these various pre-treatment processes have highlighted a good bonding behaviour, they are not environmentally friendly. These concerns can be addressed by using a laser technique to surface treat the alloy, which often results in an improved joint strength, due to an increased surface roughness, the formation of a thin oxide layer as well as a effects, such as cleaning and modification of the surface [22].

The mechanical properties of titanium-based FMLs have been studied by a number of researchers [23–25]. The tensile and fatigue properties of FMLs based on carbon fibre reinforced LARC-IAX and titanium alloy were investigated by Li and Johnson [23]. The results showed that the fatigue resistance of such FMLs is higher than that offered by the titanium alloy alone. Similar observations were made following tests on carbon fibre reinforced PEEK and titanium alloy FMLs by Cortes and Cantwell [24]. Nakatani et al. [25] studied the impact response of FMLs based on a glass fibre reinforced epoxy and a titanium alloy FML under low velocity impact. It was shown that the impact behaviour of the FMLs is dominated by fracture on the distal side of the laminate which served to reduce impact damage in the composite core.

To date, the mechanical behaviour of FMLs based on an S-glass fibre reinforced PEKK and a titanium alloy has not been examined. In principle, such a laminate should combine excellent impact resistance with a superior high-temperature mechanical capability. The aim of this study is therefore to investigate the perforation resistance of FMLs based on an S-glass fibre reinforced PEKK and a titanium alloy under different loading conditions. Firstly, the effect of increasing the surface roughness of the titanium layers is investigated through the use of a laser pre-treatment. A number of woven S-glass fibre/PEKK based titanium fibre metal laminates are then produced.

Following this, finite element models are developed to simulate the impact response of the FMLs and then validated against the corresponding experimental results. Such validated models can, in principle, be used for further parametric studies to assist in the design of high-performance FMLs.

2. Experimental procedure

2.1 Materials and sample preparation

The fibre metal laminates (FMLs) examined in this investigation were based on 0.14 mm thick layers of β -titanium alloy (15% V, 3% Al, 3% Cr, and 3% Sn) foil provided by TICOMP (California, USA) and a woven S-glass fibre reinforced PEKK (GF/PEKK) prepreg produced in-house using the manufacturing procedures described in Ref. [26]. Prior to laminating the composite and metal plies, the titanium sheets were subjected to a laser pre-treatment cycle to increase the surface roughness and enhance the strength of the bi-material interface.

Laser pre-treatment

The titanium sheets were cleaned with acetone prior to the laser treatment process and placed at the focal plane of a Nutfield XLR8-10 scan head attached to a nanosecond pulsed fibre laser (SPI 20W G4 HS L Type). The pulsed fibre laser system has a 1064 nm wavelength, a pulse duration range of 9 – 200 ns, a 20 Watt maximum average output power and a pulse repetition rate range of 25 – 500 kHz. The theoretical minimum spot size of the focused beam is approximately 50 μm . In order to modify the surface roughness of the titanium alloy, a line pattern scanning technique was used, with a hatch spacing between the scanned lines of 29 μm . A processing area of 100 x 100 mm was treated with a laser fluence of 4.09, 4.54, 5.00 and 5.45 J/cm^2 , 70 kHz pulse repetition rate, 200 ns pulse duration and a scan speed of 2.38 m/s. The scanning technique can be observed in Figure 1.

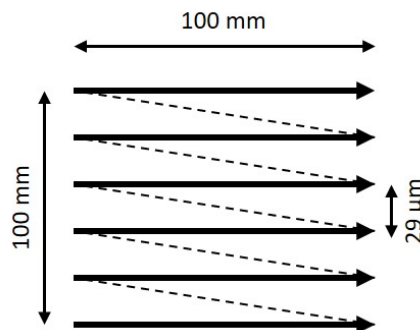


Figure 1. Schematic of the laser surface texturing scanning technique for the titanium alloy sheet.

Laminating process

A 50 μm thick film of PEKK (ARKEMA, France) was placed between the titanium layers and the GF/PEKK sheets to further enhance adhesion. The FML specimens were then manufactured by stacking the titanium alloy foils and GF/PEKK plies in a picture frame mould with dimensions of 100 mm x 100 mm. The mould was then heated in a Meyer hydraulic hot press to a temperature of 330 $^{\circ}\text{C}$ at a heating rate of approximately 3 $^{\circ}\text{C}/\text{min}$, maintained at this temperature for 30 minutes and then cooled to room temperature. A pressure of 0.5 MPa was applied to the laminates throughout the processing cycle. Details of the laminates investigated in this study are given in Table 1. Four stacking configurations were considered, ranging from a simple 2/1 laminate to a thicker 5/4 FML.

Table 1. Stacking configurations of titanium-based FMLs investigated in this study.

Laminate	Configuration	Areal density (kg/m^2)	Nominal thickness (mm)
FML (2/1)	Ti/comp/Ti	1.74	0.51
FML (3/2)	Ti/comp/Ti/comp/Ti	2.80	0.92
FML (4/3)	Ti/comp/Ti/comp/Ti/comp/Ti	4.04	1.29
FML (5/4)	Ti/comp/Ti/comp/Ti/comp/Ti/comp/Ti	5.20	1.64

Ti: titanium; comp: two plies of GF/PEKK

2.2 Mechanical tests

Tensile tests were undertaken on the titanium alloy according to ASTM E8/E8M – 16a [27]. Here, test samples were cut from the plates according to the procedures outlined elsewhere [28]. An extensometer, with a gauge length (GL) of 50 mm, was used to measure the extension of the samples during testing. The tensile tests were undertaken at a crosshead displacement rate of 0.5 mm/minute using a screw-driven Instron 3369 universal testing machine. Lap shear tests were subsequently performed to evaluate the strength of the composite-metal interface. Here, single-lap shear tests were conducted on pairs of the laser-treated titanium strips. The lap-shear samples were manufactured to ensure an overlap area of 23 x 4 mm^2 at the centre of each sample and the aforementioned PEKK film (0.1 mm thick) was used to bond the titanium strips in this region, as shown in Figure 2. The lap-shear specimens were prepared according to the DIN EN 1465 testing standard [29], suitable for testing bonds based on thermosetting adhesives. It was believed that the bond strength of the thermoplastic-based adhesive could be higher than that associated with a thermosetting adhesive. Therefore, a higher applied load would be required to fracture the specimens, possibly resulting in failure of the titanium strips rather than the joint [29]. To avoid this, the area of the joint was selected to be 23x 4 mm^2 . The strength of the lap shear specimens was measured using

the same Instron testing machine with a capacity of 50 kN. The tests were carried out at a crosshead displacement rate of 1 mm/min. Three samples were tested for each laser setting.

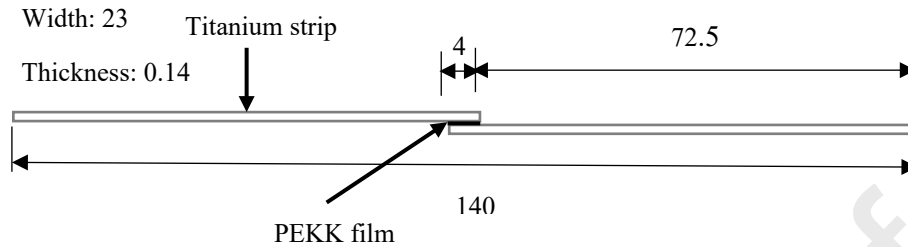


Figure 2. Schematic of the single-lap shear specimen (dimensions in mm).

Quasi-static perforation tests were conducted on 2/1, 3/2, 4/3 and 5/4 titanium-based FMLs with dimensions of 100 mm x 100 mm. The composite layers within each FML were based on two prepreg sheets. The FML plates were fixed in a 100 mm x 100 mm square frame containing an internal opening with dimensions of 72 mm x 72 mm. The plates were loaded using a hemispherical steel indenter with a diameter of 10 mm using the same Instron testing machine.

Subsequently, low velocity impact perforation tests were conducted on the titanium-based FMLs using a drop-weight tower. Here, an impact carriage with a head based on a hemispherical steel projectile similar to that used in the quasi-static perforation tests was used to load panels with dimensions of 100 mm x 100 mm, centrally. The specimens were clamped using the same frame employed for the quasi-static perforation tests. Details of the specimen stacking configurations, carriage masses and striking velocities are summarised in Table 2.

Table 2. Summary of the titanium-based FMLs subjected to low velocity impact test.

FMLs	Impactor mass (kg)	Impact velocity (m/s)
2/1 (2-ply)	1.48	4
3/2 (2-ply)	2.67	3.6
4/3 (2-ply)	3.84	3.6
5/4 (2-ply)	4.97	3.6

After testing, the samples were sectioned and polished in order to highlight the failure processes and mechanisms present within the laminates. Low magnification images (3.6x) were obtained using an optical microscope fitted

with a digital camera (Infinity 2, Lumenera Corporation). A scanning electron microscope (SEM) Type JEOL JSM 6610 SEM (Imaging Centre at the University of Liverpool) was used to investigate the surface morphology of the titanium alloy surfaces both before and after laser treatment.

3. Finite element modelling

Finite element (FE) analyses were undertaken in order to model the dynamic response of the titanium-based FMLs under low velocity impact loading. Here, finite element models were generated to closely simulate the different FML configurations considered in this study. The GF/PEKK composites were modelled as an orthotropic elastic material with 2D Hashin's failure criteria [30]. The FE model of GF/PEKK composites is detailed in Ref. [26]. The titanium alloy was modelled as an isotropic elasto-plastic material with associated damage criteria. The elastic properties of the titanium alloy are presented in Table 3. The plastic response of titanium alloy was modelled by assuming isotropic hardening. Table 4 shows the relationship between the flow stress and the plastic strain obtained from the experimental stress-strain curves.

Table 3. The elastic properties of the titanium alloy undertaken in this work.

Material	Density (kg/m ³)	Young's modulus (GPa)	Poisson's ratio
Titanium alloy (Ti-15-3-3-3-β)	4760	100	0.33

Table 4. The plastic properties of the titanium alloy investigated in this study.

Titanium alloy (Ti-15-3-3-3-β)	
Plastic strain	Yield stress (MPa)
0	1000
0.0304	1015
0.0311	1030
0.0318	1045
0.0326	1060
0.0333	1070
0.0341	1080
0.0367	1100
0.0394	1110
0.0438	1120
0.0454	1122

Ductile and shear damage models, available in ABAQUS/Explicit [31], were used to model damage initiation within the titanium layers. The failure strain obtained experimentally from the uniaxial tensile tests was taken as the fracture strain at which the onset of the damage occurs. The ductile and shear damage parameters, i.e. stress triaxiality, shear stress ratio and strain rate, were requested where the tensile and shear failure occurred. Again, the fracture strain was obtained from the true strain-stress curves obtained following the uniaxial tensile tests. Following damage initiation in these metallic layers, an effective element-based plastic displacement was adopted to model subsequent damage evolution. The interfaces between the titanium and composite layers within the FMLs were simulated using cohesive elements based on a nominal stress and energy defined in terms of traction-separation. Table 5 summarises the material properties of the cohesive layer that were used in this study.

Table 5. Material properties of the cohesive layer [32].

$k_{nn}=k_{ss}=k_{tt}$	t_n^0	t_s^0	t_t^0	G_{Ic}	G_{IIc}	G_{IIIc}
10^{14}	61	68.4	68.4	1564	2113	2113
N/m ³	MPa	MPa	MPa	J/m ²	J/m ²	J/m ²

A plate size of 72 mm x 72 mm with fully-fixed edges as boundary conditions was considered in the simulations. Given the symmetry in geometric and loading conditions, only one half of the specimen was modelled, as shown in Figure 3. The initial velocity was applied to the projectile in the normal direction to the target.

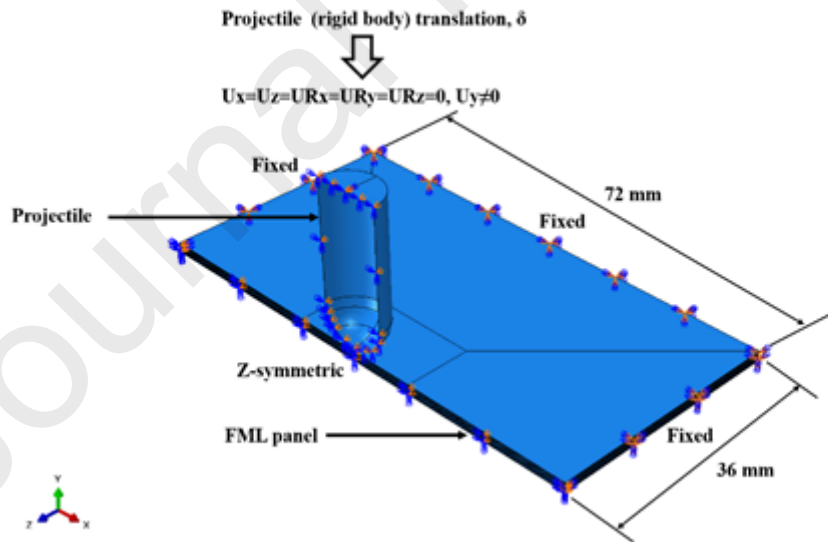


Figure 3. The mesh, loading and boundary conditions of the half-model of FMLs plates.

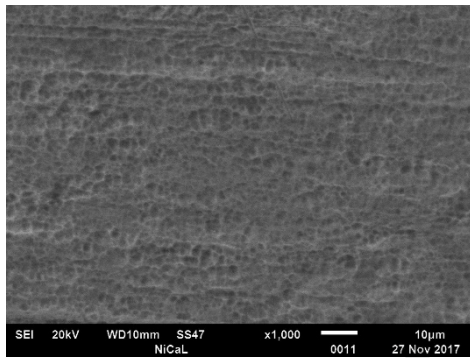
Eight-noded continuum shell elements (SC8R) along with 2D Hashin's failure criteria were applied to the composite plies in the FMLs. Eight-noded solid brick elements (C3D8R) with reduced integration and hourglass control were used to mesh the titanium layers. Interaction between the layers in the FMLs was defined as a general

contact interaction, and surface-to-surface (contact pair) interaction was employed between the projectile surface and the node-set in the target central region of each layer. The interfaces between the titanium and composites layers were modelled using eight-noded 3D cohesive elements (COH3D8).

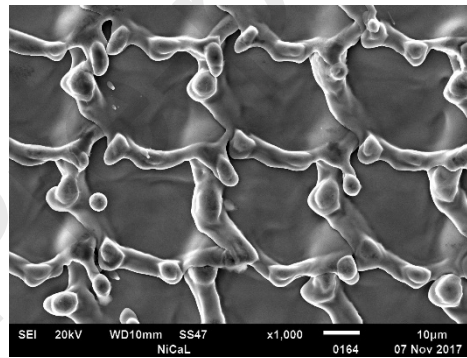
4. Results and Discussion

4.1 Surface characterization of the untreated and treated titanium alloy foils

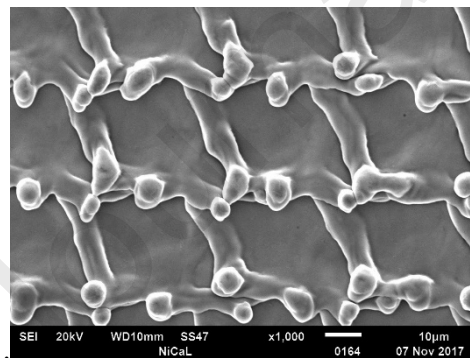
Figure 4 shows SEM images of the β -titanium alloy subjected to different levels of laser fluence. Included is an example of an untreated alloy. The magnification in all images is similar in order to facilitate comparisons. It is clear that increasing the laser fluence serves to increase the roughness of the titanium alloy. A higher laser power generates a coarser texture on the sample surface compared to that observed in the virgin sample. With increasing laser fluence, the degree of material removal and the depth of the micro pits clearly increases.



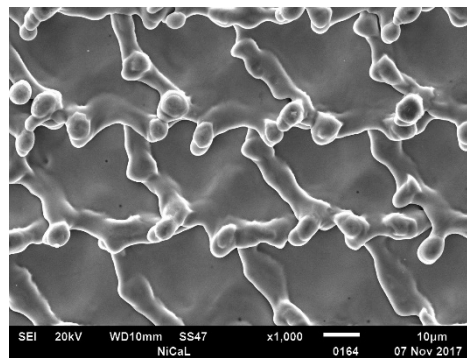
(a) Laser fluence = untreated



(b) Laser fluence = 4.09 J/cm²



(c) Laser fluence = 4.54 J/cm²



(d) Laser fluence = 5.00 J/cm²

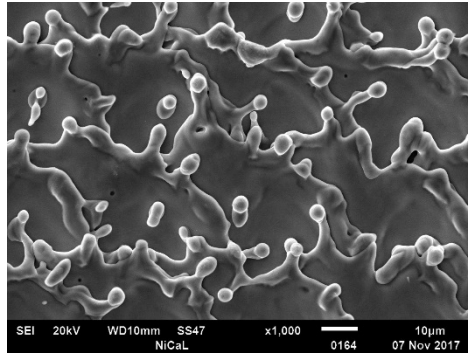
(e) Laser fluence = 5.45 J/cm²

Figure 4. SEM images of the titanium alloy following a laser surface treatment at different laser fluences.

The surface roughness of the β -titanium alloy was characterized by a white light interferometer optical profiling system (Wyko NT1100). Measurements for each of the different laser fluence were performed in order to obtain the average surface roughness (R_a) characterisation presented in Table 6.

Table 6. Average surface roughness of the β -titanium alloy.

Titanium alloy (Ti-15-3-3-3- β)	
	Average Roughness (R_a)
As-received sample	309.14 nm
4.09 J/cm ² fluence	1.19 μ m
4.54 J/cm ² fluence	1.43 μ m
5.00 J/cm ² fluence	1.63 μ m
5.45 J/cm ² fluence	1.72 μ m

Tensile tests were conducted on the 140 micron thick titanium foils following the laser surface treatments outlined in Figure 4. The results show that the tensile strength of the titanium alloy decreases slightly with increasing laser fluence. For example, the average tensile strength of the untreated foil was 1122 MPa, whereas that for the foils subjected to a fluence of 5.45 J/cm² was 1069 MPa, representing a reduction of approximately five percent. This reduction in tensile strength is likely to be due to the fact that the laser treatment process not only removes surface material, but also acts to anneal the foil.

Figure 5 summarises the lap-shear strength values of samples based on the laser-treated titanium foils and the PEKK film. The figure can be divided into two regions, these being, Region I where the lap-shear strength increases with increasing surface roughness of the titanium foil, reaching of approximately 31 MPa at a surface roughness of 1.43 μ m. This can be attributed to the formation of a microporous structure on the treated surface

which filled with the resin, resulting in a good metal-resin bond. In Region II, the lap-shear strength remains roughly constant, suggesting that the maximum value has been achieved and that further increases in laser fluence would have little effect. Based on these observations, a laser fluence of 4.54 J/cm^2 was used to treat the titanium foils investigated in the remaining part of this study.

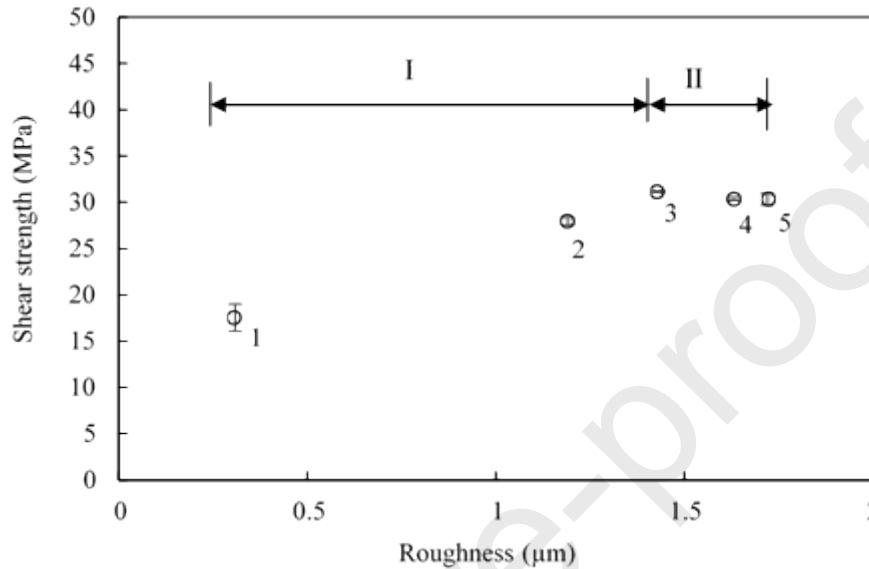


Figure 5. The variation of shear strength as a function of surface roughness showing the effect of different laser treatments.

1 = untreated, 2 = Laser fluence = 4.09 J/cm^2 , 3 = Laser fluence = 4.54 J/cm^2 , 4 = Laser fluence = 5.0 J/cm^2 and 5 = Laser fluence = 5.45 J/cm^2

4.2 Quasi-static perforation of the titanium based-FMLs

The perforation resistance of the four titanium-based FMLs was evaluated by conducting a series of quasi-static tests on a universal testing machine. Typical load-displacement traces following tests on the 2/1, 3/2, 4/3 and 5/4 fibre metal laminates are shown in Figure 6. An examination of the figure indicates that the load-displacement traces exhibit similar trends, with the load increasing in a non-linear fashion up to a maximum value, before the initiation of damage associated with a tension/shear fracture in the lowermost titanium alloy layer of the target. Following the maximum in the load-displacement trace, damage developed within the volume of the material as the indenter penetrates the target, resulting in a progressive drop in the contact force. It is evident from the figure that increasing the thickness of the FML results in a higher peak force, as well as a higher stiffness. For example, the FML based on the 5/4 stacking configuration exhibits a peak force of 4490 N, which is almost three times of that offered by the 2/1 FML.

The energy absorbed by each laminate during the perforation process was established by determining the area under the load-displacement trace. Figure 7 shows the variation of the energy absorbed by the four FML configurations considered here. It is clear from the figure that the energy required to perforate these FMLs increases with target thickness, a similar observation to that made elsewhere [33]. The energy required to perforate the 5/4 FML is approximately three times of that required to perforate the 2/1 FML. However, the residual displacement of the latter is higher than that of the former due to higher membrane deformation of the much thinner laminate.

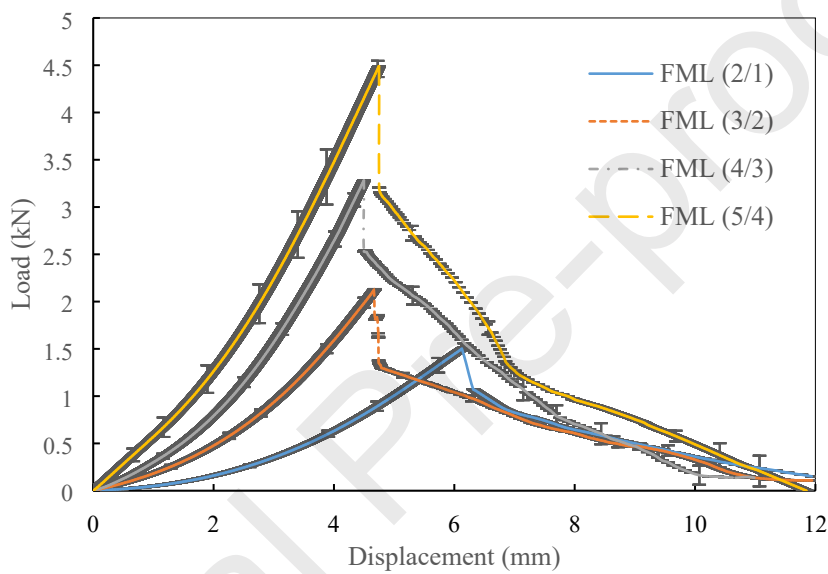


Figure 6. Load-displacement traces following quasi-static perforation tests.

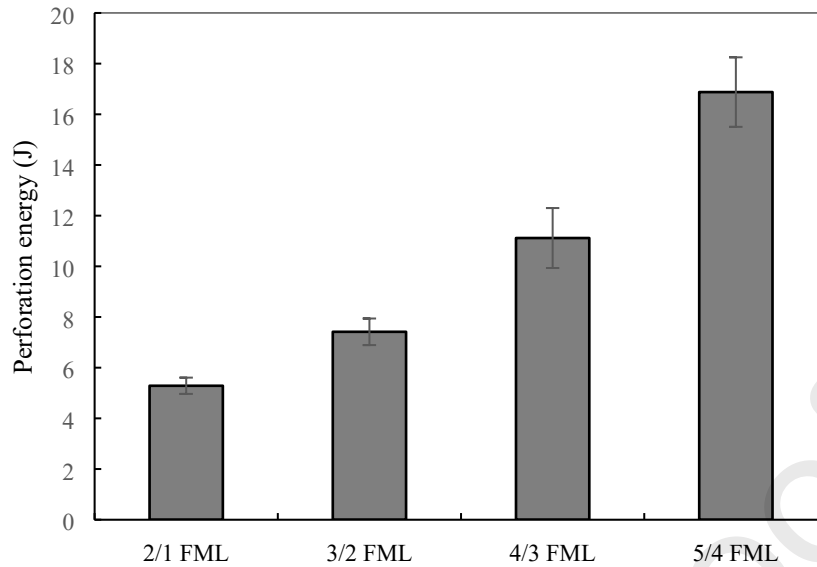


Figure 7. Perforation energies of the 2/1, 3/2, 4/3 and 5/4 FMLs.

4.3 Low velocity impact response of the titanium-based FMLs

Load-displacement traces for the 2/1, 3/2, 4/3 and 5/4 titanium-based FMLs following low velocity impact loading are shown in Figure 8. Here, all specimens exhibit a similar response where the impact force increasing to a maximum value before damage initiation occurs. The force then decreases rapidly after this point. Clearly, the traces are similar to those obtained following quasi-static perforation testing. However, the peak forces under dynamic loading were slightly higher than the corresponding quasi-static values, suggesting a level of strain rate-sensitivity in these hybrid materials.

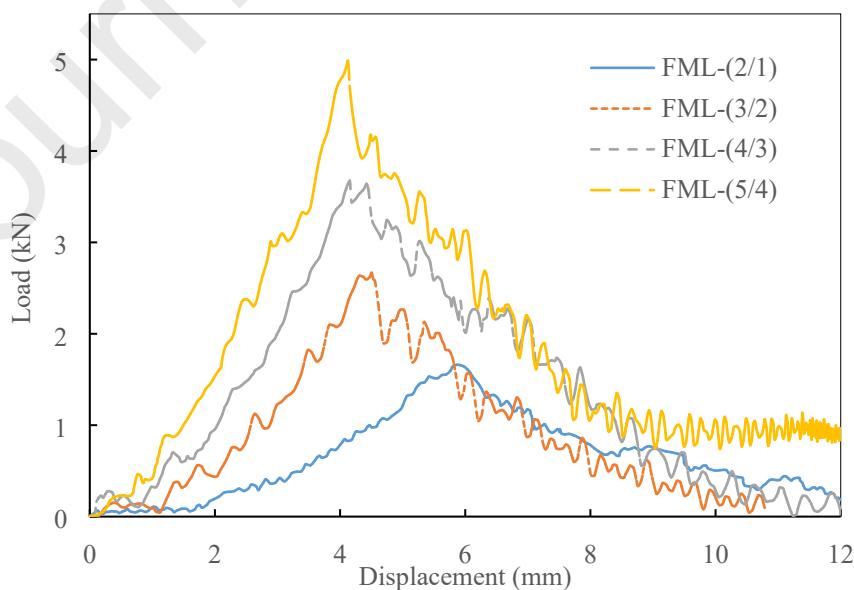


Figure 8. Load-displacement traces following low velocity impact tests.

In order to further investigate the rate-sensitivity of these laminates, the dynamic peak forces in Figure 8 are compared to the corresponding quasi-static values in Figure 6 and the results are shown in Figure 9, where it is clear that the dynamic peak forces are higher than those under quasi-static loading. Similarly, the dynamic values of absorbed energy are plotted against the quasi-static values, as shown in Figure 10. Once again, the impact-loaded FMLs exhibit a higher level of energy absorption than those subjected to quasi-static perforation testing.

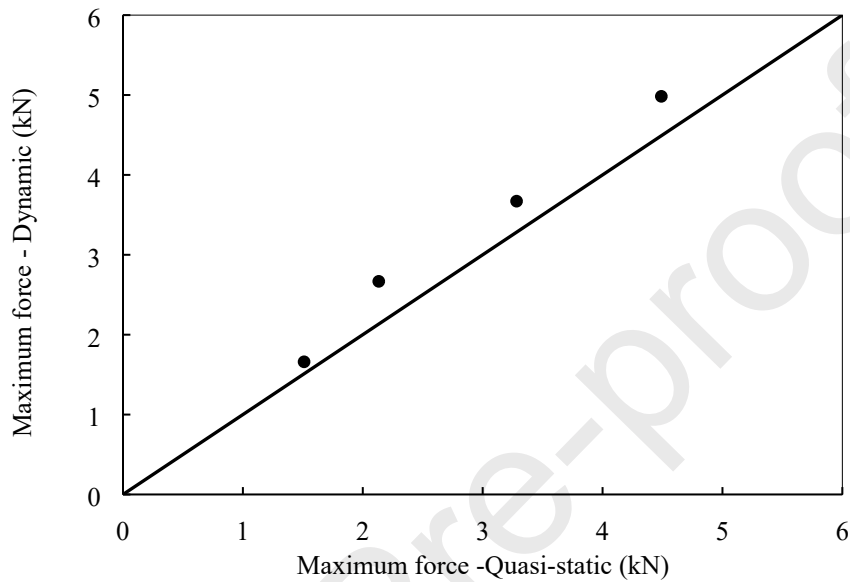


Figure 9. Comparison of the maximum force following quasi-static and dynamic loading for the 2/1, 3/2, 4/3, and 5/4 stacking configurations.

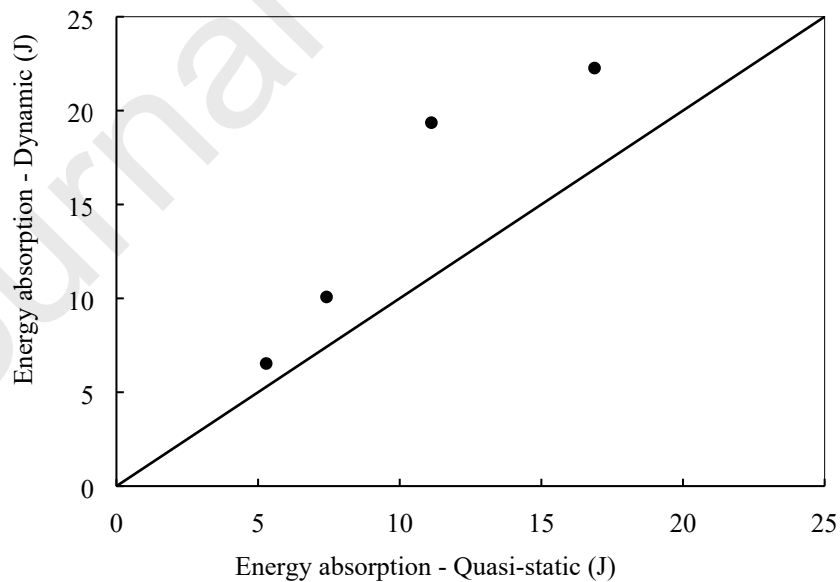


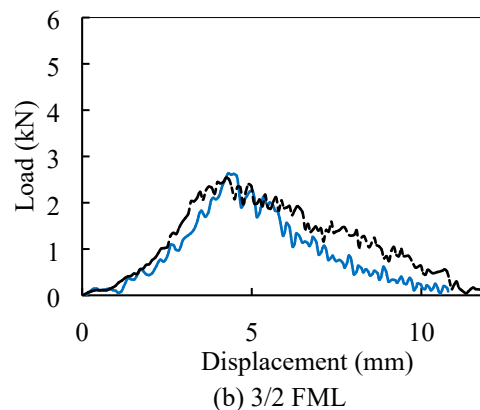
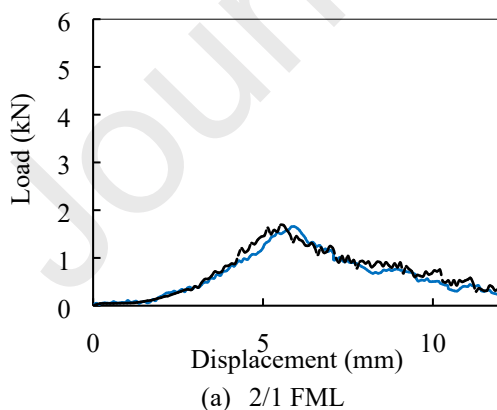
Figure 10. Comparison of the perforation energy following quasi-static and dynamic loading for the 2/1, 3/2, 4/3 and 5/4 stacking configurations.

4.4 The finite element modelling outputs

Finite element models based on ABAQUS/Explicit were used to predict the perforation resistance of the titanium-based FMLs under impact loading. As before, four stacking configurations were considered in this part of the investigation.

Figure 11 compares the numerical and experimentally-measured load-displacement traces for the FML panels subjected to impact by a 10 mm diameter hemispherical projectile. From the figure, it is clear that the numerical results show good agreement with the experimental data. During impact loading, the predicted and measured traces exhibit an oscillatory response, due to the dynamic nature of the test. The FE models slightly over-estimate the stiffnesses of the panels as a result of the assumption of fully-fixed boundary conditions at four edges of the target in the model. The predicted peak loads for the 2/1, 3/2, 4/3 and 5/4 FMLs are approximately 1690, 2540, 3600 and 5000 Newtons, respectively, data that compare favourably with the measured values of 1660, 2670, 3670 and 4980 Newtons. The differences between the two sets of values correspond to only 1.7, 4.7, 1.9 and 0.4 %, respectively.

The penetration stage of the impact event, a phase during which the projectile passes through the target and the impact force decreases following peak load, was accurately captured by the finite element models. The numerical values of displacement at peak load exhibit discrepancies of 6.0, 5.7, 1.9 and 2.5 % relative to the corresponding experimental data. It is worth noting that the FE models succeed in predicting the trends in the displacement at peak loads, whereby the displacement decreases with increasing panel thickness. The differences between the predicted perforation energies and the associated experimental data are 9.5, 19, 3.9 and 12.2 %, respectively.



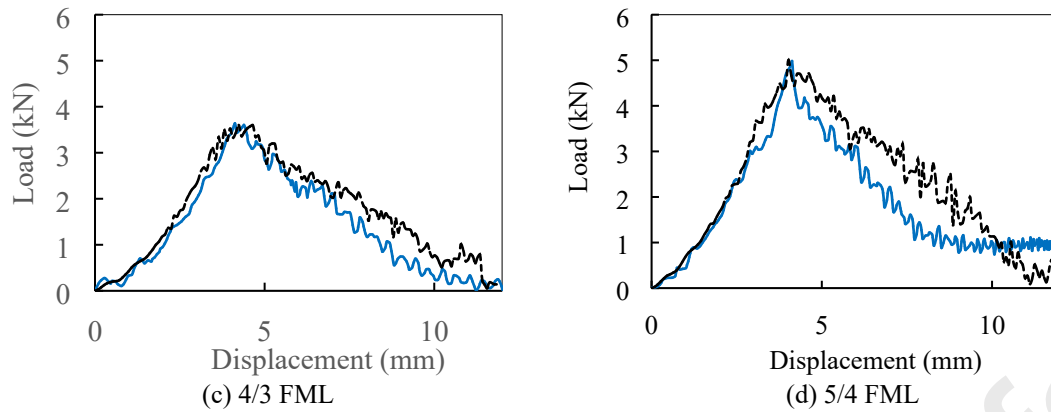


Figure 11. Load-displacement traces following low velocity impact loading. The solids lines correspond to experimental traces and the dashed lines to numerical predictions.

Figure 12 compares the predicted and experimental failure modes in the FMLs investigated following perforation. It can be seen that the predicted rear surface profiles are similar in appearance to those observed following the impact tests. The principal experimentally-observed failure mode (i.e. the cross-shaped fracture pattern on the rear surfaces) is captured reasonably well by the FE models. Although there is some discrepancy between the predicted and experimental failure modes for the 2/1 FMLs, the failure modes were successfully simulated for the three remaining FML panels.

Figure 13 compares the predicted and experimental cross-sections of the titanium-based FMLs investigated in this study. Clearly, the FE models are capable of predicting the basic features of the failure modes obtained experimentally, in terms of local deformations in the centre of the plate, delamination between the adjacent layers, interlaminar damage and the cross-shaped cracks on the rear surfaces of the FMLs investigated herein. An examination of the figures indicates that the rear surface cracks are slightly longer in the FE models than that in the experimental tests. The images for the FE models were captured with the projectile remaining inside the target and this was not the case for the test panels. Moreover, the predicted thickness of the FMLs in the crack tip region is less than that observed experimentally, which is likely to be due to the use of continuum shell elements for simulating the composite layers in which an empty space exists between the shell skins.

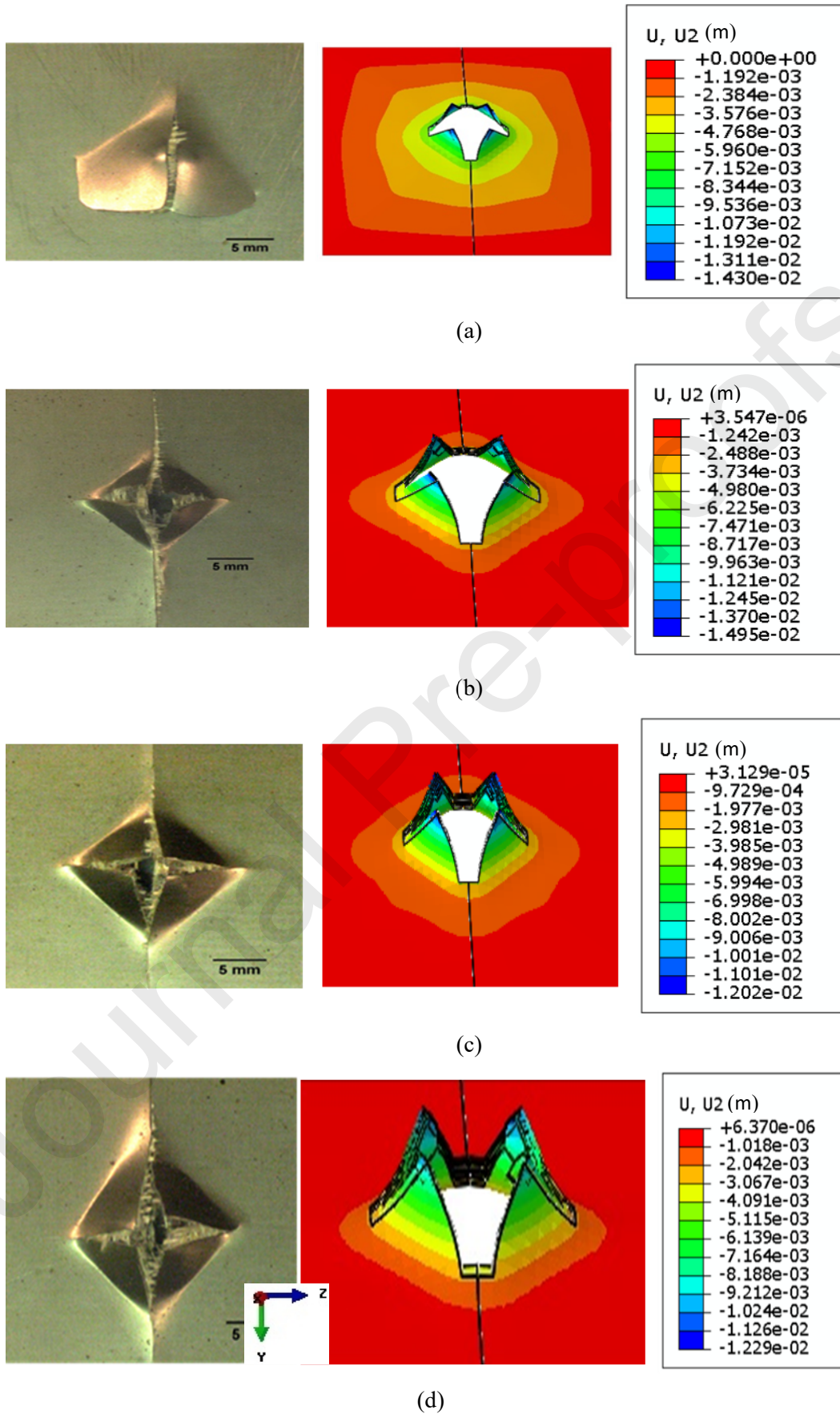
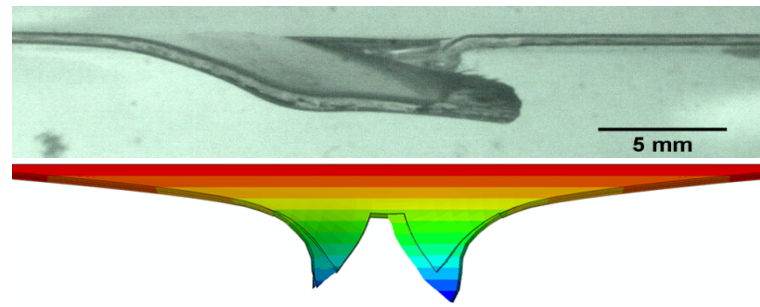
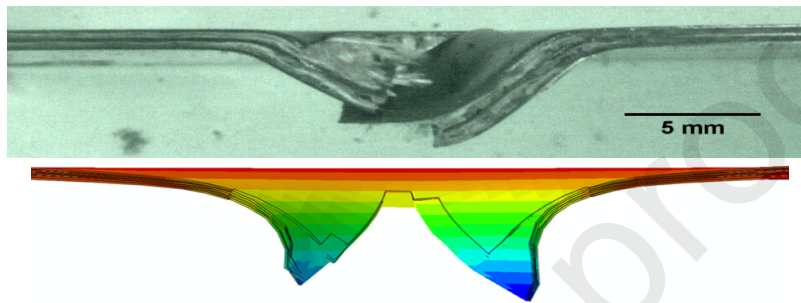


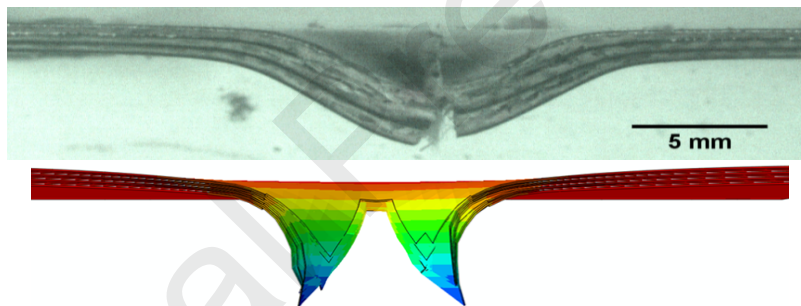
Figure 12. Failure modes in the: (a) 2/1; (b) 3/2; (c) 4/3; (d) 5/4 FMLs.



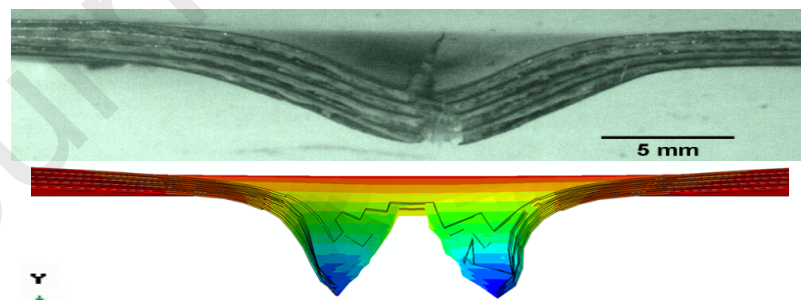
(a) 2/1 FML



(b) 3/2 FML



(c) 4/3 FML



(d) 5/4 FML

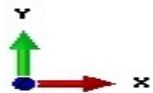


Figure 15. Comparison of the experimental and predicted failure modes in the FMLs.

5 Conclusions

The mechanical properties of FMLs based on a titanium alloy and glass fibre reinforced PEKK have been investigated. Initially, the influence of a laser pre-treatment on the bond strength between the plain composites and the titanium alloys was evaluated. Here, it was shown that a laser fluence of 4.54 J/cm^2 yields an optimum bonding strength between the constituent materials. Tests were subsequently undertaken to investigate the perforation resistance of the FMLs at both quasi-static and dynamic rates of strain. Here, a strain-rate sensitive response was observed with the perforation energy increasing as the loading rates pass from the quasi-static to dynamic conditions. The perforation response of the FMLs investigated was subsequently modelled using finite element analysis techniques. The FE models provided an accurate simulation of the perforation resistance of the titanium-based FMLs for the range of stacking sequences considered. The models yielded reasonable predictions of the maximum force, maximum displacement, perforation energy and also identified the correct failure modes within the targets.

Acknowledgment

The authors would like to thank ARKEMA Company for providing the PEKK film.

Data availability

The raw/processed data required to reproduce these findings cannot be shared at this time due to technical or time limitations.

References

- [1] A. Asundi A. and Alta Y.N. Choi, Fibre metal laminates: an advanced material for future aircraft, *J. Mater. Process. Technol.*, vol. 63, pp 384–394, 1997.
- [2] E. Hombergmeier. Development of advanced laminates for aircraft structures. Proceedings of 25th International Congress of the Aeronautical Sciences. 3-8 September, Hamburg, Germany, 2006.
- [3] A. Vlot, “Low-velocity impact loading on fibre reinforced aluminium laminates (ARALL and GLARE) and other aircraft sheet materials.” Delft University of Technology, 1993.
- [4] A. Vlot, Impact loading on fibre metal laminates, *Int. J. Impact Eng.*, vol. 18, pp. 291-307, 1996.
- [5] G. V Reyes and W. J. Cantwell, “The mechanical properties of fibre -metal laminates based on glass fibre reinforced polypropylene,” *Compos. Sci. Technol.*, vol. 60, pp. 1085–1094, 2000.

- [6] J. Zhou, The energy-absorbing behaviour of novel aerospace composite structures, PhD Thesis, University of Liverpool, 2015.
- [7] N.G. Gonzalez-Ganche, E.A. Flores-Johnson, P. Cortes and J.G. Carrillo, "Evaluation of surface treatments on 5052-H32 aluminum alloy for enhancing the interfacial adhesion of thermoplastic-based fiber metal laminates," *Int. J. Adhesion & Adhesives.*, vol. 82, pp. 90–99, 2018.
- [8] V. Babrauskas and R. D. Peacock, "Heat release rate: The single most important variable in fire hazard," *Fire Safety Journal*, vol. 18. pp. 255–272, 1992.
- [9] G. T. Linteris and I. P. Rafferty, "Flame size, heat release, and smoke points in materials flammability," *Fire Saf. J.*, vol. 43, pp. 442–450, 2008.
- [10] A. P. Mouritz, Z. Mathys, and A. G. Gibson, "Heat release of polymer composites in fire," *Compos. Part A Appl. Sci. Manuf.*, vol. 37, pp. 1040–1054, 2006.
- [11] P. Olivier, J. P. Cottu, and B. Ferret, "Effects of cure cycle pressure and voids on some mechanical properties of carbon/epoxy laminates," *Composites*, vol. 26, pp. 509–515, 1995.
- [12] P. Cortés and W. J. Cantwell, "The prediction of tensile failure in titanium-based thermoplastic fibre-metal laminates," *Compos. Sci. Technol.*, vol. 66, pp. 2306–2316, 2006.
- [13] T. Sinmazçelik, E. Avcu, M. Ö. Bora, and O. Çoban, "A review: Fibre metal laminates, background, bonding types and applied test methods," *Mater. Des.*, vol. 32, pp. 3671–3685, 2011.
- [14] P.-Y. B. Jar, R. Mulone, P. Davies, and H.-H. Kausch, "A study of the effect of forming temperature on the mechanical behaviour of carbon-fibre/peek composites," *Compos. Sci. Technol.*, vol. 46, pp. 7–19, 1993.
- [15] H. E. N. Bersee, "Composite aerospace manufacturing processes," *Encycl. Aerosp. Eng.*, pp. 1–16, 2010.
- [16] M. H. Salek, "Effect of processing parameters on the mechanical properties of carbon/PEKK thermoplastic composite materials," Master diss., Concordia University, Canada, 2005.
- [17] P. Molitor, V. Barron, and T. Young, "Surface treatment of titanium for adhesive bonding to polymer composites: a review," *Int. J. Adhes. Adhes.*, vol. 21, pp. 129–136, 2001.
- [18] C. Y. Guo, A. T. Hong Tang, J. K. Hon Tsoi, and J. P. Matinlinna, "Effects of different blasting materials on charge generation and decay on titanium surface after sandblasting," *J. Mech. Behav. Biomed. Mater.*,

- vol. 32, pp. 145–154, 2014.
- [19] B. R. Chrcanovic, N. L. C. Leão, and M. D. Martins, “Influence of different acid etchings on the superficial characteristics of Ti sandblasted with Al₂O₃,” *Mater. Res.*, vol. 16, pp. 1006–1014, 2013.
- [20] P. He, K. Chen, and J. Yang, “Surface modifications of Ti alloy with tunable hierarchical structures and chemistry for improved metal-polymer interface used in deepwater composite riser,” *Appl. Surf. Sci.*, vol. 328, pp. 614–622, 2015.
- [21] T. Mertens *et al.*, “Investigation of surface pre-treatments for the structural bonding of titanium,” *Int. J. Adhes. Adhes.*, vol. 34, pp. 46–54, 2012.
- [22] A. Kurtovic, E. Brandl, T. Mertens, and H. J. Maier, “Laser induced surface nano-structuring of Ti-6Al-4V for adhesive bonding,” *Int. J. Adhes. Adhes.*, vol. 45, pp. 112–117, 2013.
- [23] E. Li and W. S. Johnson, “An Investigation into the Fatigue of a Hybrid Titanium Composite Laminate,” *J. Compos. Technol. Res.*, vol. 20, pp. 3–12, 1998.
- [24] P. Cortes and W. J. Cantwell, “The tensile and fatigue properties of carbon fiber-reinforced PEEK-Titanium fiber-metal laminates,” *J. Reinf. Plast. Compos.*, vol. 23, pp. 1615–1623, 2004.
- [25] H. Nakatani, T. Kosaka, K. Osaka, and Y. Sawada, “Damage characterization of titanium/GFRP hybrid laminates subjected to low-velocity impact,” *Compos. Part A Appl. Sci. Manuf.*, vol. 42, pp. 772–781, 2011.
- [26] N. Nassir, R. S. Birch, W. J. Cantwell, Q. Y. Wang, L. Q. Liu, and Z. W. Guan, “The perforation resistance of glass fibre reinforced PEKK composites,” *Polym. Test.*, vol. 72, no. September, pp. 423–431, 2018.
- [27] ASTM E8/E8M – 16a, “Standard test methods for tension testing of metallic materials,” 2016.
- [28] P. Verleysen, I. De Baere, and J. Degrieck, “Pre-fatigue influence on quasi-static tensile properties of Ti-6Al-4V in thin-sheet form,” *EDP Sci.*, vol. 6, pp. 3–9, 2010.
- [29] “DIN EN 1465:2009 Adhesives - Determination of tensile lap-shear strength of rigid-to-rigid bonded assemblies.”
- [30] Z. Hashin and A. Rotem, “A Fatigue Criterion for Fiber-Reinforced Materials,” *J. Compos. Mats*, vol. 7, pp. 448–464, 1973.

- [31] Dassault Systèmes Simulia, “Analysis User’s Guide,” *Abaqus 6.14*, 2014.
- [32] W. Tan and B. G. Falzon, “Modelling the nonlinear behaviour and fracture process of AS4/PEKK thermoplastic composite under shear loading,” *Compos. Sci. Technol.*, vol. 126, pp. 60–77, 2016.
- [33] J. Fan, Z. W. Guan, and W. J. Cantwell, “Numerical modelling of perforation failure in fibre metal laminates subjected to low velocity impact loading,” *Compos. Struct.*, vol. 93, pp. 2430–2436, 2011.

Highlights

- Quasi-static and Impact perforation of titanium-based fibre metal laminates
- A laser fluence of 5.54 J/cm^2 on the titanium layers gives a good bond strength
- Finite element modelling of perforation failure of the FMLs
- Good correlation between the experimental and simulated results
- Capture load-displacement traces and failure modes of the FMLs

Journal Pre-proofs